Capsule membranes encapsulated with smart nanogels for facile detection of trace lead(II) ions in water

Wen-Ying Liu[a], Xiao-Jie Ju[a,b,*], Yousef Faraj[a,b], Fan He[a], Han-Yu Peng[a], Yu-Qiong Liu[a], Zhuang Liu[a,b], Wei Wang[a,b], Rui Xie[a,b], Liang-Yin Chu[a,*]

[a] *School of Chemical Engineering, State Key Laboratory of Hydraulics and Mountain River Engineering, Sichuan University, Chengdu, Sichuan 610065, China*

[b] *State Key Laboratory of Polymer Materials Engineering, Sichuan University, Chengdu, Sichuan 610065, China*

*Corresponding authors at: School of Chemical Engineering, Sichuan University, Chengdu, Sichuan, 610065, China.

E-mail addresses: juxiaojie@scu.edu.cn (X.-J. Ju); chuly@scu.edu.cn (L.-Y. Chu).

Abstract

A novel method based on capsule membranes encapsulated with smart nanogels is successfully developed for facilely detecting trace lead(II) (Pb^{2+}) ions, which are hazardous to both human health and the environment because of their toxicity. The capsule membrane system is composed of a semi-permeable calcium alginate membrane and encapsulated poly(*N*-isopropylacrylamide-*co*-acryloylamidobenzo-18-crown-6) (PNB) nanogels. The semi-permeable membrane allows Pb^{2+} ions and water to pass through quickly, but rejects the encapsulated nanogels and polymers totally. As soon as Pb^{2+} ions appear in the aqueous environment and enter into the capsule, they can be specifically recognized by encapsulated PNB nanogels via forming 18-crown-6/Pb^{2+} complexes that cause a Pb^{2+}-induced phase transition of PNB nanogels from hydrophobic to hydrophilic state. As a result, the osmotic pressure inside the capsule membrane increases remarkably, and thus the elastic capsule membrane isothermally swells upon the presence of Pb^{2+} ions in the environmental aqueous solution. The Pb^{2+}-induced swelling degree of the capsule membrane is dependent on the concentration of Pb^{2+} ions ($[Pb^{2+}]$) in water. Thus, the $[Pb^{2+}]$ value in water is able to be easily detected by directly measuring the Pb^{2+}-induced isothermal swelling ratio of the capsule membrane, which we demonstrate by using 15 prepared capsule membranes arranged in a line. The Pb^{2+}-induced swelling ratios of the capsule membrane groups are easily observed with the naked eye, and the detection limit of the $[Pb^{2+}]$ in water is 10^{-9} mol L^{-1}. Such a proposed method provides an easy and efficient strategy for facile detection of trace threat analytes in water.

Keywords

Capsule membranes; Smart nanogels; Lead(II) ions; Facile detection; Ion-recognizable phase transition

1. Introduction

Lead(II) (Pb^{2+}) ion is a toxic heavy metal ion and hazardous environmental pollutant, which tends to bio-accumulation. Excessive Pb^{2+} ion intake results in disorders, malfunction and malformation of organs and various pathologies including carcinogenesis [1-4]. One of the main sources of Pb^{2+} ion intake is drinking water containing trace concentration of Pb^{2+} ions, which can be simplified to [Pb^{2+}]. For example, the Flint drinking water crisis in the state of Michigan in USA happened in 2016 because of Pb^{2+} ions leaching from water pipes into the drinking water, caused over 100,000 residents to suffer from elevated blood lead levels [5-7]. Therefore, development of effective technologies for facilely detecting [Pb^{2+}] in water is very important for human health and environmental protection.

Up to now, inductively coupled plasma spectrometry [8, 9], atomic absorption spectrometry [10, 11] and electrochemical methods [12] have been successfully used to detect the [Pb^{2+}] in water. However, these methods could not meet the requirement of facile detection of [Pb^{2+}] because of some inherent limitations such as the complicated and non-portable instrument as well as the need of professional operation. Recently, several strategies have been developed to detect [Pb^{2+}] based on Pb^{2+}-recognition response of stimuli-responsive materials [13, 14] by converting [Pb^{2+}] into different signals, such as flowrate signals [15-18], electrical signals [19, 20] and optical signals [21-26]. The most typically used Pb^{2+}-responsive polymeric materials are copolymers with 18-crown-6 crown ether moieties acting as Pb^{2+} receptors and poly(*N*-isopropylacrylamide) (PNIPAM) acting as backbones. Stable host-guest complexes can be formed by specific identification of the 18-crown-6 moieties in the copolymers to Pb^{2+} ions [27]. Using such Pb^{2+}-responsive copolymers, micro-cantilever beam [26], hydrogel gratings [28, 29], micro-valves [15-18] and thermometer-like devices [30] have been developed for detection of [Pb^{2+}]. Micro-cantilever beams and hydrogel gratings respectively convert the signals of Pb^{2+}-

induced hydrogel volume swelling into the optical signal changes of laser deflection [26] or grating diffraction efficiency [28, 29]. Both methods with micro-cantilever beams and hydrogel gratings require to be equipped with optical systems, which restrict their applications for facile detection of [Pb^{2+}]. Gating membranes [16-18] and microchips [15] with micro-valves for detection of [Pb^{2+}] have been developed by converting the [Pb^{2+}] signals into the changes of flowrates. However, these methods still require precise systems for measuring the change of flowrates, which certainly hinder the practical applications for facile detection of [Pb^{2+}]. Recently, a thermometer-like device has been developed for visual detection of [Pb^{2+}] by converting the [Pb^{2+}] signals into the changes of liquid length in a microchannel [30]. Although this method could be employed for simple detection of [Pb^{2+}], the minimum concentration that can be detected is quite high (10^{-3} mol L^{-1}), which is 10^5 times higher than the maximum [Pb^{2+}] value that allowable for drinking water as the World Health Organization provided (*i.e.*, 4.83×10^{-8} mol L^{-1}). Consequently, for facilely detecting trace [Pb^{2+}] in water, the development of efficient methods still remains challenging.

Here, we report on a novel method based on capsule membranes encapsulated with smart nanogels for facilely detecting trace [Pb^{2+}] in water (**Fig. 1**). The capsule membrane system is composed of a semi-permeable membrane and encapsulated smart nanogels that functionalized with 18-crown-6 crown ether units for specifically recognizing Pb^{2+} ions (**Fig. 1a**). The semi-permeable membrane is made of calcium alginate (Ca-Alg), and the materials of nanogels are poly(*N*-isopropylacrylamide-*co*-acryloylamidobenzo-18-crown-6) (PNB). The semi-permeable membrane allows Pb^{2+} ions and water to pass through quickly, but totally rejects the encapsulated nanogels and polymers to pass through. As soon as Pb^{2+} ions appear in the aqueous environment and enter into the capsule membrane, they can be specifically captured by the 18-crown-6 moieties in PNB nanogels, which result in the formation of stable positively charged 18-crown-

6/Pb^{2+} complexes [15-18]. Such host-guest complexations increase the electrostatic repulsion between charged B18C6Am/Pb^{2+} complexes and cause a Pb^{2+}-induced isothermal phase changing of the encapsulated PNB nanogels that changing from shrunken and hydrophobic state to swollen and hydrophilic state (**Fig. 1b,c**). Due to hydrophobic-to-hydrophilic phase change of the PNB nanogels encapsulated inside the capsule membrane, the osmotic pressure inside the capsule membrane increases remarkably. As a result, the water molecules enter into the capsule from outside, and thus the elastic Ca-Alg capsule membrane isothermally swells upon the appearance of Pb^{2+} ions in the environmental aqua-solution until osmotic equilibrium is reached inside and outside the capsule membrane (**Fig. 1b**). As the Pb^{2+}-induced phase transition of PNB is dependent on the [Pb^{2+}] value [15-18], the isothermal swelling degree of the capsule membrane is also dependent on the [Pb^{2+}] value. Thus, through simply measuring the Pb^{2+}-induced isothermal swelling ratio of the proposed capsule membrane, the [Pb^{2+}] in water is able to be easily detected. To amplify the Pb^{2+}-induced swelling effect, several capsule membranes can be arranged in a line, so that the Pb^{2+}-induced increase of the total length of the capsule membrane group can be simply detected with naked eyes. In this study, as a demonstration, a group of 15 prepared capsule membranes are used to detect the [Pb^{2+}] in water, within a variation range of [Pb^{2+}] value being 10^{-6} ~ 10^{-9} mol L^{-1}, and the quantitative relationship between the Pb^{2+}-induced swelling ratio of total length of the capsule membrane group and the [Pb^{2+}] is established. The proposed strategy based on capsule membranes in this work provides a facile method and an easily portable tool for detecting trace [Pb^{2+}] in water.

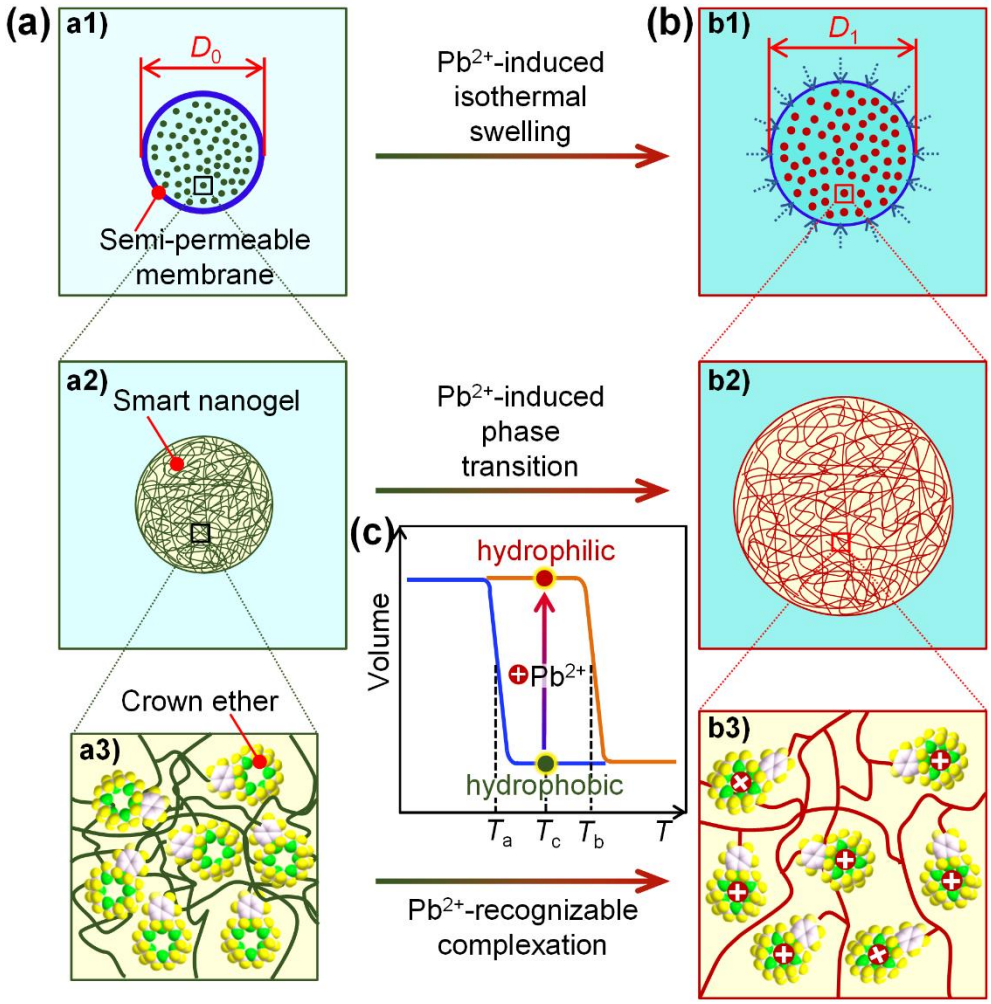

Fig. 1. Diagrammatic sketch of the proposed concept of a capsule membrane system for facilely detecting Pb^{2+} ions in water. The capsule membrane system (a) is composed of a semi-permeable membrane (a1) and encapsulated smart nanogels (a2) that functionalized with 18-crown-6 crown ether units (a3) for specifically recognizing Pb^{2+} ions. Isothermal swelling of the capsule membrane is induced by the appearance of Pb^{2+} ions in the environmental aqua-solution (b), because of the Pb^{2+}-induced increase of osmotic pressure inside the core compartment of capsule membrane (b1). The nanogels encapsulated inside the capsule membrane exhibit a Pb^{2+}-induced isothermally hydrophobic-to-hydrophilic phase changing (c, a2→b2) on account of the formation of host-guest complexes between 18-crown-6 and Pb^{2+} (a3→b3), leading to the increase of osmotic pressure inside the capsule. Thus, the Pb^{2+} ions in water are able to be easily detected by directly observing the swelling of capsule diameter (D_0 → D_1).

2. Experimental section

2.1. Materials

A mixture consisted of hexane and acetone was used to recrystallize *N*-isopropylacrylamide (NIPAM, 98%, TCI). By employing a previously used method [31], 4′-nitro-benzo-18-crown-6, which was got from TCI with 98% content, was used to prepare 4′-Amino-benzo-18-crown-6 ($AmB_{18}C_6$). The dehydration catalyst 1-(3-(dimethylamino) propyl)-3-ethyl carbodiimide hydrochloride (EDC) was bought from Sigma-Aldrich. Other chemical reagents including ammonium persulfate (APS), sodium alginate (Na-Alg), *N,-N*′-methylene-bis-acrylamide (MBA), sodium carboxymethylcellulose (Na-CMC), sodium dodecyl sulfate (SDS), calcium nitrate ($Ca(NO_3)_2$) and acrylic acid (AAc) were bought from Chengdu Kelong Chemicals with analytical grade. Deionized (DI) water (18.2 MΩ·cm, 25 °C) was made by a Millipore Milli-Q Plus system.

2.2. Synthesis and characterizations of PNB nanogels with Pb^{2+}-responsiveness

The Pb^{2+}-responsive PNB nanogels that were encapsulated into the capsule membranes were prepared by using the precipitation copolymerization method with NIPAM and AAc (**Fig. 2**), and then by modification with $AmB_{18}C_6$ according to a previously reported method [18]. Briefly, to synthesize PNB nanogels, poly(*N*-isopropylacrylamide-*co*-acrylic acid) (PNA) nanogel samples were firstly synthesized by dissolving monomers of AAc (0.4324 g) and NIPAM (2.7158 g), surfactant of SDS (0.0091 g), initiator of APS (0.0685 g) and cross-linker of MBA (0.1203 g) into a round-bottom flask with 300 mL of deionized water (**Fig. 2a,b**). In order to achieve complete removal of dissolved oxygen, the above described solution was bubbled for 30 min by using nitrogen gas. And then, the reaction was underway for 4 h at 70 °C in the flask that was sealed off with nitrogen atmosphere. At the end of the reaction, ice-bath was used to cool down the

obtained solution to room temperature. Furthermore, filtration and dialysis were carried out to achieve a purified PNA nanogel suspension. Finally, PNB nanogels were synthesized by grafting $AmB_{18}C_6$ onto the PNA nanogels with catalysis of EDC for dehydration reaction (**Fig. 2b,c**).

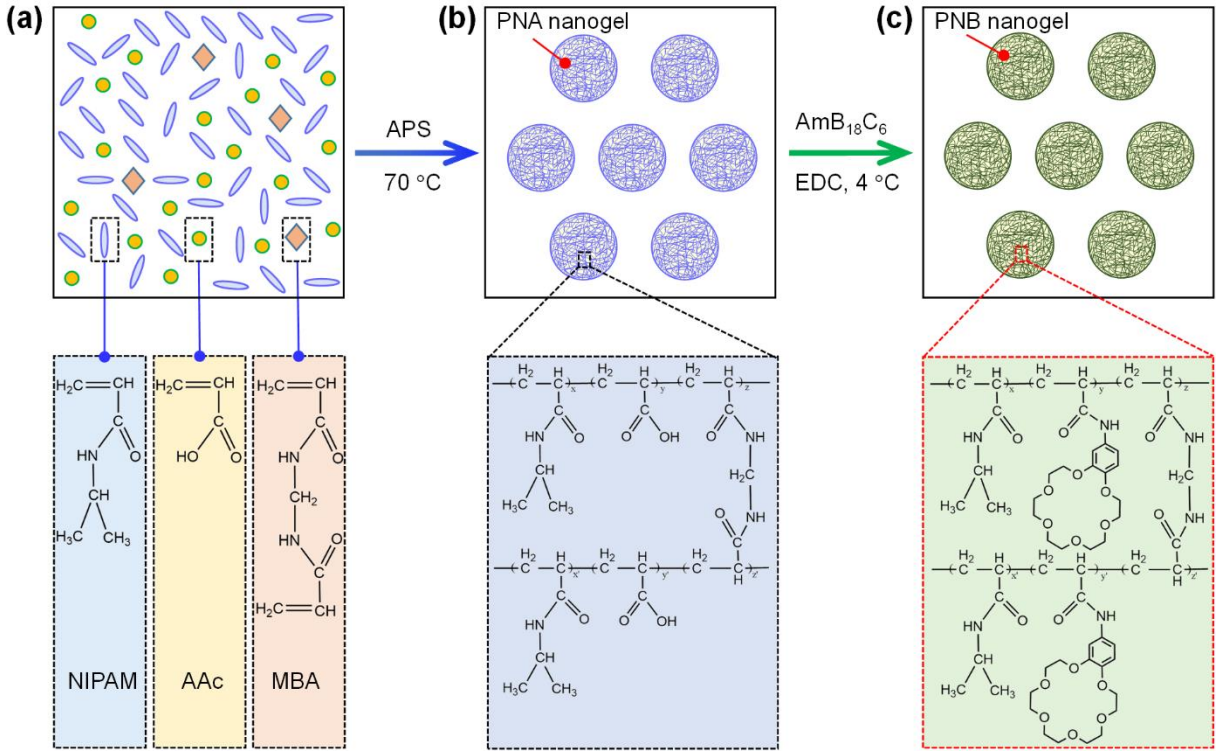

Fig. 2. The syntheses of PNA and PNB nanogels. The Pb^{2+}-responsive PNB nanogels are prepared by using the precipitation copolymerization method with NIPAM and AAc as monomers, MBA as cross-linker and APS as initiator to synthesize PNA nanogels firstly (a,b), and followed by modification with $AmB_{18}C_6$ for the formation of PNB nanogels with catalysis of EDC for dehydration reaction between carboxyl groups in PNA nanogels and amino groups in $AmB_{18}C_6$ monomers (b,c).

For characterization of chemical compositions, a Fourier transform infrared spectroscope (FT-IR, Thermo Scientific, NICOLET iS50) was used. By using a field-emission scanning

electron microscope (FESEM, JEOL, JSM-7500F), the morphology of PNB nanogels after freeze-drying was obtained. The samples of PNB nanogels for FESEM characterization were prepared by sputter-coated with gold after drying them at room temperature.

For investigation of Pb^{2+}-responsive performance of the PNB nanogels, a dynamic light scattering instrument (DLS, Malvern, Zetasizer Nano ZEN3690) was used to measure the [Pb^{2+}]-dependent changes of the diameters of PNB nanogels in aqua-solutions with a temperature range of 20 ~ 65 °C. The PNB nanogel-containing dispersion was highly diluted using deionized water and equilibrated for at least 180 s at each temperature that was predetermined. The [Pb^{2+}] values in water were varied as 0, 5×10^{-4}, and 5×10^{-3} mol L^{-1}.

2.3. Fabrication of capsule membranes

For preparation of the capsule membranes, water-in-water (W/W) droplets that acted as templates were prepared by a co-extrusion mini-fluidic capillary technology [32] (**Fig. 3a**), which can accurately and independently control the inner and outer phase fluids, so as to accurately control the size of droplet templates for synthesizing capsule membranes with good monodispersity. Briefly, a cylindrical capillary tube was used to sleeve a square capillary tube to build a coaxial geometry, in which the inner diameter for the cylindrical tube is 2.0 mm, and the outer dimension for the square capillary tube is 1.4 mm. The nested square tube was longer than cylindrical capillary tube at the injection side (inlet) but shorter at the other end (outlet). To get a cylindrical cone (nozzle) at the end of the square tube, its outlet was heated under an alcohol burner. The formation of W/W droplets was occurred at the outlet of the above described device by simultaneously injecting the inner fluid containing PNB nanogels (**Fig. 3b,c**) and Na-CMC (0.75% w/v) into the square tube and the outer fluid containing Na-Alg (2% w/v) and SDS (1% w/v) through the space between the cylindrical and square tubes with two injection pumps. The

formed W/W droplets continuously dripped into a $Ca(NO_3)_2$ solution (15% w/v) to fabricate capsule membranes encapsulated with nanogels via Ca^{2+}-induced crosslinking of alginate in the outer fluid (**Fig. 3d**). For the complete removal of the residual chemicals, washing was performed for the prepared capsule membranes with pure water, followed by storing them in pure water (**Fig. 3e**) for subsequent experiments.

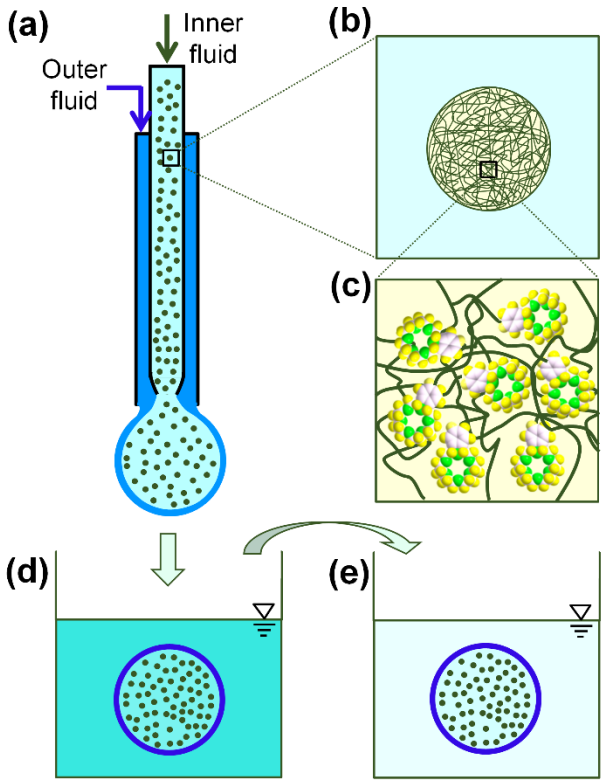

Fig. 3. Preparation of the proposed capsule membranes. A co-extrusion minifluidic device is used to fabricate water-in-water (W/W) droplet templates (a), in which the inner aqueous phase contains PNB nanogels (b) that functionalized with 18-crown-6 units (c) and the outer aqueous phase contains Na-Alg. The capsule membranes form immediately as the W/W droplet templates drip into $Ca(NO_3)_2$ solution (d) via Ca^{2+}-induced crosslinking of alginate. Washing of the capsule membranes was carried out by pure water, followed by storing them in pure water (e).

A digital camera was used to take an optical micrograph of the capsule membranes, and an analysis software was used for measuring their diameters. The membrane thickness (δ) and size distribution (CV) of the capsule membranes were respectively obtained with the following equations [32]:

$$CV = 100\% \times \left(\sum_{i=1}^{N} \frac{(D_i - \overline{D_n})^2}{N-1} \right)^{1/2} / \overline{D_n} \quad (1)$$

$$\delta = \frac{\overline{D_n}}{2} \left[1 - \left(\frac{Q_i/Q_o}{1+Q_i/Q_o} \right)^{1/3} \right] \quad (2)$$

where D_i denotes the diameter of the ith capsules [mm], $\overline{D_n}$ denotes the arithmetic average diameter [mm], N denotes the total number of the capsule membranes counted, and Q_o and Q_i are respectively denote the volumetric flowrates of outer fluid and inner fluid [mL h^{-1}].

2.4. Facile detection of [Pb^{2+}] with the capsule membranes encapsulated with nanogels

A home-made glass device for facile detection of [Pb^{2+}] with capsule membranes was assembled with a heating jacket, which is connected with a constant-temperature system to regulate the solution temperature inside the device. A certain number of nanogel-encapsulated capsule membranes were placed into the glass device in a line. Typically, 15 capsule membranes were used as a group in the experiments. The glass device was equipped with a graduated scale, and thus the total length of the capsule membrane group could be directly observed by the naked eye.

For determination of the optimal operation temperature (T_c) of the capsule membranes for Pb^{2+}-detection, effect of temperature on volume swelling performance of the capsule membranes was evaluated. The temperature, at which Pb^{2+}-induced volume swelling extent of the capsule membranes was the most significant, was defined as the optimal operation temperature. To

demonstrate the detection of [Pb^{2+}], solutions containing Pb^{2+} with different concentrations were substituted for pure water around the capsule membranes inside the glass device. The variation range of [Pb^{2+}] values was 10^{-9} ~ 10^{-6} mol L^{-1}. For each [Pb^{2+}] value, equilibrium time for the capsule membranes was at least 30 min at each temperature that was predetermined. To obtain the temperature-dependent swelling performance of the capsule membranes, the equilibrated total lengths of the capsule membrane group, with the variation range of temperature being 23 ~ 50 °C, were observed directly by the naked eye.

To test and verify the capsule membranes with high selectivity for [Pb^{2+}]-detection, the changes of the total lengths of the capsule membrane group in aqueous solutions containing different ions (K^+, Na^+, Sr^{2+} and Ba^{2+}) were also measured. In these experiments, the ion concentration of each ionic solution was 10^{-9} mol L^{-1}. The length change ratio (R_L) of the capsule membrane group, which was caused by ions including Pb^{2+} ions, is evaluated by following equation:

$$R_L = \frac{L_{ion} - L_{H_2O}}{L_{H_2O}} \times 100\% \quad (3)$$

where L_{ion} and L_{H_2O} respectively denote the total lengths of the capsule membrane group in ion-containing solution and pure water.

Effect of the content of PNB nanogels encapsulated in the capsule membranes on the Pb^{2+}-induced swelling performances of capsule membranes was also investigated. Capsule membranes were fabricated with inner fluids containing different concentrations of PNB nanogels (5, 10, 16, 20, and 26 mg mL^{-1}). A certain number of capsule membranes encapsulated with different amounts of PNB nanogels were put into the glass device containing pure water and equilibrated at T_c. After that, aqua-solution with [Pb^{2+}] = 10^{-9} mol L^{-1} was substituted for pure water at the fixed temperature of T_c.

To demonstrate the facile Pb^{2+}-detection, the swelling performances of capsule membranes in aqueous solutions with different [Pb^{2+}] values at optimal operation temperature were investigated using the glass device. The capsule membranes in the glass device were equilibrated for 2 h in pure water firstly. Then, the pure water in the glass device was replaced by aqueous solutions containing Pb^{2+} ions. The change of the total length of capsule membrane group in the glass device after switching from pure water to Pb^{2+}-containing solution was measured and recorded at each 10 min, until the equilibrium of osmotic pressures existed between inside and outside of the capsule membranes was achieved.

3. Results and discussion

3.1. Chemical compositions and morphological characteristics of PNB nanogels

Fig. 4a exhibits the FT-IR spectra of the characterized nanogels of both PNA and PNB. Because of the existence of the isopropyl groups of NIPAM, appearance of the double peaks at 1387 cm^{-1} and 1366 cm^{-1}in both PNA and PNB nanogels is observed, demonstrating that the PNIPAM backbones are existed in these nanogels. Meanwhile, the characteristic peak for the carboxylic groups of PNA nanogels at 1715 cm^{-1} is disappeared after modifying with $AmB_{18}C_6$, confirming that the carboxylic groups are converted in the reaction of EDC condensation. Furthermore, in spectrum of PNB nanogels, the C=C skeletal stretching vibration of phenyl ring, both of the C-O symmetric and asymmetric stretching vibrations of Ar-O-R, and C−O−C asymmetric stretching vibration of R−O−R′, are appeared at the characteristic peaks of 1130, 1057, 1285 and 1517 cm^{-1} respectively, demonstrating the successful synthesis of PNB nanogels. Moreover, uniform spherical shapes of PNB nanogels are achieved, and the average diameter is about 430 nm in dried state (**Fig. 4b**).

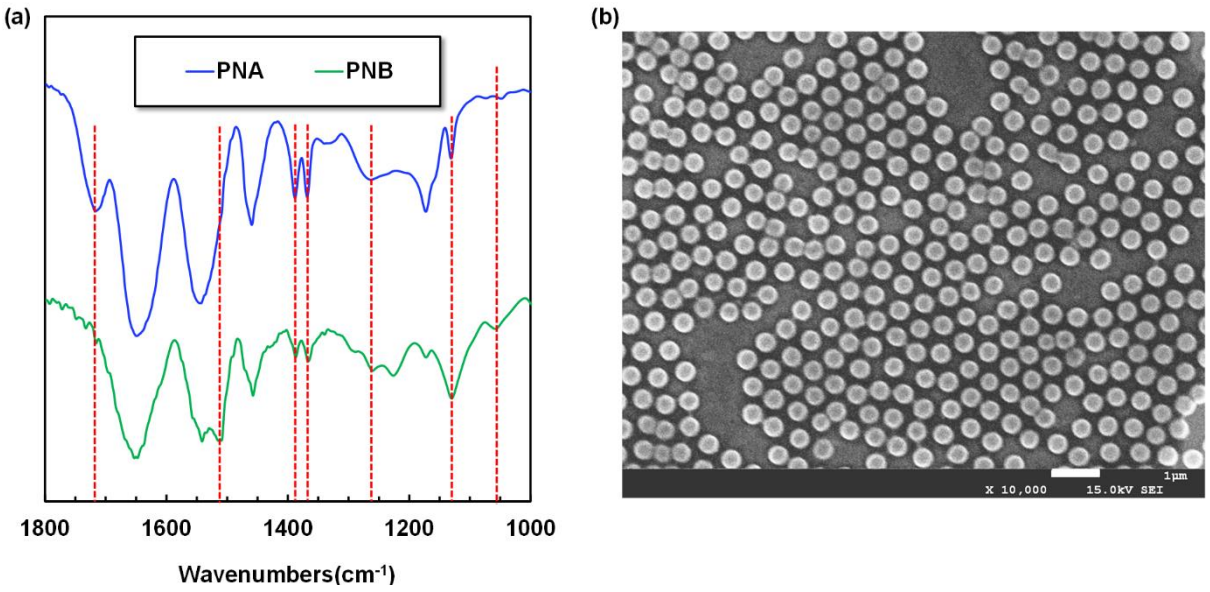

Fig. 4. Characterizations of composition and morphology for nanogels. (a) The characterization results of PNA (blue) and PNB (green) nanogels with FT-IR spectra. (b) FESEM microphoto for PNB nanogels.

3.2. Performances of PNB nanogels with Pb^{2+}-responsiveness

Because of the existence of PNIPAM backbones with thermo-responsive property, the PNB nanogels exhibit thermo-responsive volume changes in pure water ($[Pb^{2+}] = 0$ mol L^{-1}) and Pb^{2+}-containing solutions. As shown in Fig. 5a, the hydrodynamic diameters of PNB nanogels decrease with increasing the temperature, owing to the thermo-induced dehydration effect of the PNIPAM networks decreases the hydrophilicity of PNB nanogels. As the temperature increases across the volume phase transition temperature (VPTT), the hydrodynamic diameter of PNB nanogels decreases sharply. For the VPTT of PNB nanogels, it changes to higher temperatures in Pb^{2+}-containing solutions compared to that in pure water owing to the Pb^{2+}-induced isothermal hydrophobic-to-hydrophilic phase transition on account of the formation of B18C6Am/Pb^{2+} host-guest complexes, resulting in the Pb^{2+}-recognition-responsive performances of PNB nanogels [31,

33, 34]. Notably, owing to the Pb^{2+}-induced phase transition of PNB nanogels changing from hydrophobic state to hydrophilic state, the average diameter of PNB nanogels exhibits an increasing trend with increasing [Pb^{2+}] from 0 mol L^{-1} to 5×10^{-3} mol L^{-1} at any fixed temperature below 55 °C. Due to the formation of stable positively charged B18C6Am/Pb^{2+} host-guest complexes, the hydrogen bonds between hydrophilic groups in PNB nanogels and water molecules are strengthened. As a result, PNB nanogels undergo an isothermal hydrophobic-to-hydrophilic transition and suffer a Pb^{2+}-induced volume swelling due to electrostatic repulsion between these charged groups. With the increase of [Pb^{2+}], more B18C6Am/Pb^{2+} complexes can be formed in PNB nanogels, thus the electrostatic repulsion among charged B18C6Am/Pb^{2+} complexes is further enhanced. Therefore, the nanogel networks become more hydrophilic and looser, so that more water molecules can be adsorbed into the nanogels, making the nanogels swell more. When PNB nanogels are encapsulated into the capsule membranes, such phase transition of PNB nanogels induced by Pb^{2+} ions enables the conversion of [Pb^{2+}] signal into the size change of capsule membranes. The Pb^{2+}-induced diameter change ratio, $D_{Pb^{2+}}/D_{H_2O}$, is used to evaluate the diameter swelling extent of PNB nanogels upon responding to Pb^{2+} ions at a given temperature. $D_{Pb^{2+}}$ and D_{H_2O} are denotations of the nanogel diameters in solution that contains Pb^{2+} ions and in pure water respectively. With the increase of temperature, the values of $D_{Pb^{2+}}/D_{H_2O}$ of PNB nanogels in solutions that contain Pb^{2+} ions increase first during the temperature increases within a range of 20 ~ 38 °C. However, when the temperature is further increased from the beginning of 38 °C to the finishing of 65 °C, the values of $D_{Pb^{2+}}/D_{H_2O}$ of PNB nanogels decrease (**Fig. 5b**). These results indicate that there exists a most significant change of Pb^{2+}-induced diameter swelling ratio of PNB nanogels at 38°C, which could be the optimal operation temperature for the detection. The largest value of $D_{Pb^{2+}}/D_{H_2O}$ at 38 °C means that the

PNB nanogels can achieve the most significant phase transition upon responding to [Pb^{2+}] changes at this temperature. When [Pb^{2+}] values are 5×10^{-4} and 5×10^{-3} mol L^{-1}, Pb^{2+}-induced swelling ratios of diameters of PNB nanogels are 1.58 and 1.88, respectively.

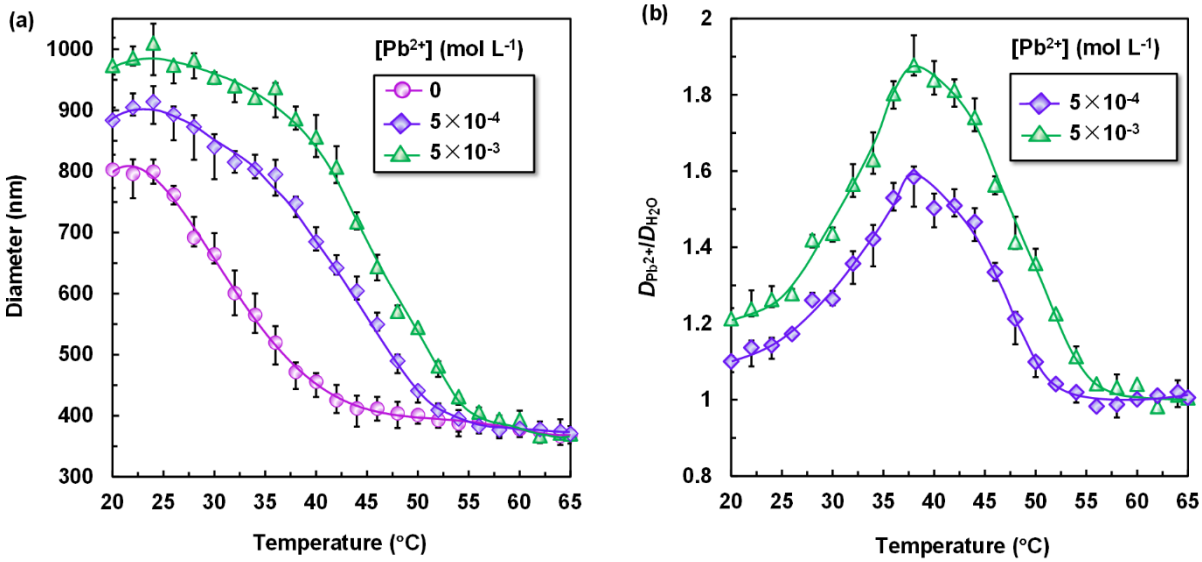

Fig. 5. The changes of hydrodynamic diameter (a) and $D_{Pb^{2+}}/D_{H_2O}$ value (b) of PNB nanogels when [Pb^{2+}] is 0, 5×10^{-4} and 5×10^{-3} mol L^{-1} at different temperatures.

3.3. Morphological analyses of capsule membranes

The ratio of volumetric flowrate of inner phase (Q_i) to volumetric flowrate of outer phase (Q_o) directly affects the membrane thickness (δ) of the capsule membranes (**Fig. 6a**). To obtain an appropriate thickness of the capsule membrane, Q_o is fixed at 10 mL h^{-1} and Q_i is changed from 5 to 300 mL h^{-1} in this study. Membrane thickness of the capsule membrane decreases with increasing the ratio of Q_i/Q_o. In order to avoid the rupture of the capsule membranes during Pb^{2+}-induced swelling, the capsule membranes in the subsequent experiments are fabricated with Q_i = 60 mL h^{-1} and Q_o = 10 mL h^{-1}. The photograph and size distribution of prepared capsule

membranes encapsulated with PNB nanogels show that the capsule membranes are featured with uniform spherical shapes with narrow size distribution (**Fig. 6b**). The average diameter of the capsule membranes is 3.75 mm, with *CV* value being 2.44%. With calculation by Eq. (2), the average thickness of the membrane is about 95 μm. The size distribution of the capsule membranes might affect the detection results, because the capsule membranes with different sizes contain different contents of encapsulated PNB nanogels. Therefore, at the same Pb^{2+} concentration, the Pb^{2+}-induced size changes of the capsule membranes with different sizes are different. For capsule membranes with wide size distributions, the detecting deviation may be large. Such a good monodispersity of the capsule membranes prepared in this study could minimize the effect of capsule size on the repeatability of the detection. Furthermore, to minimize detection system errors of a single capsule, the detection signal of [Pb^{2+}] is amplified by arranging several capsules in a line.

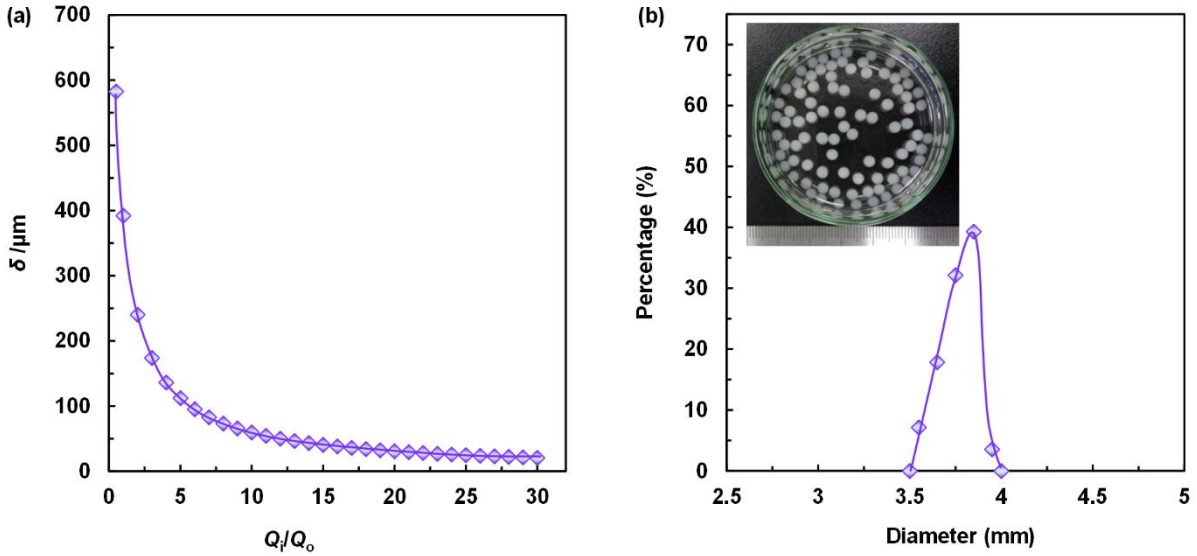

Fig. 6. Thicknesses and diameters of capsule membranes. (a) The relationship between thickness of capsule membranes (δ) and the flowrate ratio (Q_i/Q_0). (b) The size distribution and typical photograph (the inset) of capsule membranes encapsulated with PNB nanogels.

3.4. Optimal temperature for Pb^{2+}-detection using capsule membranes

For determination of the optimal temperature for Pb^{2+}-detection using the prepared capsule membranes, effect of temperature on the swelling of the capsule membranes induced by Pb^{2+} ions are investigated. The relationship between the Pb^{2+}-induced length change ratio (R_L) of the capsule membrane group and the temperature can be obtained (**Fig. 7**). For the nanogel-encapsulated capsule membranes in Pb^{2+}-containing solutions, the maximum value of R_L appears at 38 °C, which is the same as the optimal operation temperature for the PNB nanogels. Furthermore, at a fixed temperature, the R_L values of the capsule membranes increase with increasing the $[Pb^{2+}]$. At 38 °C, the R_L values are respectively 8.33%, 25%, 28.33% and 30% corresponding to the Pb^{2+} concentrations of 10^{-9}, 10^{-8}, 10^{-7} and 10^{-6} mol L^{-1}. In the subsequent experiments, the operation temperature is selected as 38 °C.

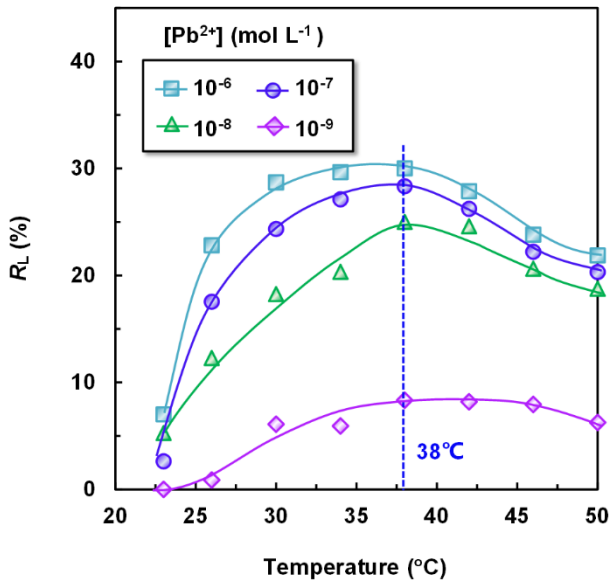

Fig. 7. Influence of temperature on Pb^{2+}-induced length change ratio of the capsule membrane group upon switching the environmental solution from pure water to Pb^{2+}-containing solutions.

3.5. Selectivity of nanogel-encapsulated capsule membranes for detection of Pb^{2+}

The selective performances of nanogel-encapsulated capsule membranes for detection of Pb^{2+} are investigated by introducing various interfering ions, including Na^+, K^+, Sr^{2+} and Ba^{2+}, which are featured with relatively large inclusion stability constants between them and 18-crown-6 crown ethers among divalent and monovalent ions [15], as the detection mechanism of capsules for Pb^{2+} is mainly based on the supramolecular complexation between 18-crown-6 moieties of PNB nanogels and Pb^{2+} ions via forming host-guest complexes and the Pb^{2+}-induced phase transition of nanogels. The concentrations of the interfering ions are the same as that of Pb^{2+} (10^{-9} mol L^{-1}). Those results show that the ion-induced length change ratios (R_L) of the capsule membrane groups in response to Na^+, K^+, Sr^{2+}, Ba^{2+} and Pb^{2+} ions are respectively 0.82%, 1.64%, 2.46%, 3.28% and 13.33% at 38 °C (**Fig. 8**). Obviously, the swelling ratios of capsule membranes induced by the interfering ions are much less than that induced by Pb^{2+}. For the value of inclusion stability constant (K) of 18-crown-6 crown ethers that complexed with metal ions, it has been reported that it is ordered as $Pb^{2+} > Ba^{2+} > Sr^{2+} > K^+ > Na^+$ in water (Pb^{2+}: K=18621 M^{-1}; Ba^{2+}: K=7413 M^{-1}; Sr^{2+}: K=525 M^{-1}; K^+: K=107 M^{-1}; Na^+: K=6.3 M^{-1}) [33, 35-37]. The inclusion complex constant between 18-crown-6 and Pb^{2+} is much larger than other ions; thus, the PNB nanogels can specifically recognize Pb^{2+} by forming B18C6Am/Pb^{2+} complexes with high stability and enhance the Pb^{2+}-induced phase transition of nanogels. Therefore, the resultant swelling ratio of capsule membranes induced by Pb^{2+} is the largest one among those ions. The results confirm the excellent selectivity of the proposed nanogel-encapsulated capsule membranes for detection of Pb^{2+} ions.

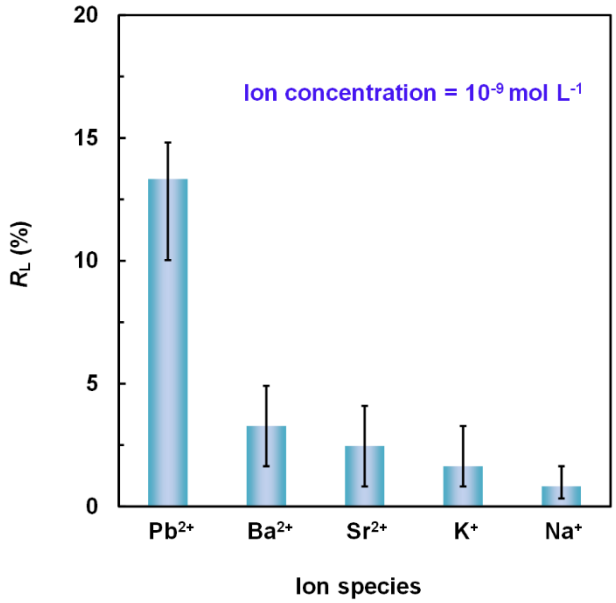

Fig. 8. Ion-induced length change ratios (R_L) of the capsule membrane groups in response to Na^+, K^+, Sr^{2+}, Ba^{2+} and Pb^{2+}. T = 38 ℃.

3.6. Effect of the contents of PNB nanogels inside capsules on the Pb^{2+}-induced swelling ratios of capsule membranes

Pb^{2+}-induced swelling performance of the prepared capsule membranes is driven by the increase of the osmotic pressure inside the capsules, which is induced by the Pb^{2+}-responsive phase transition of encapsulated PNB nanogels. To confirm this point, the swelling properties of blank capsule membranes without encapsulated PNB nanogels are also investigated, and the results show that nearly no swellings of blank capsule membranes without encapsulated PNB nanogels are observed upon adding Pb^{2+} in the water. Therefore, the conversion of [Pb^{2+}] signal into the Pb^{2+}-induced increase of osmotic pressure inside capsule membranes is directly affected by the content of encapsulated PNB nanogels. In the experiments, almost all of the capsule membranes containing different amounts of PNB nanogels have the same total lengths in pure water (**Fig. 9a**). However, when 10^{-9} mol L^{-1} Pb^{2+} ions present in the solution, the total lengths

of the capsule membrane groups increase with increasing the contents of encapsulated PNB nanogels. Therefore, the length change ratios of the capsule membrane groups increase when the contents of encapsulated PNB nanogels increase (**Fig. 9b**). However, it is worth mentioning that the capsule membranes may rupture in the operation processes if they swell too much. Therefore, the content of PNB nanogels encapsulated inside capsule membranes is selected as 10 mg mL^{-1} for the subsequent experiments.

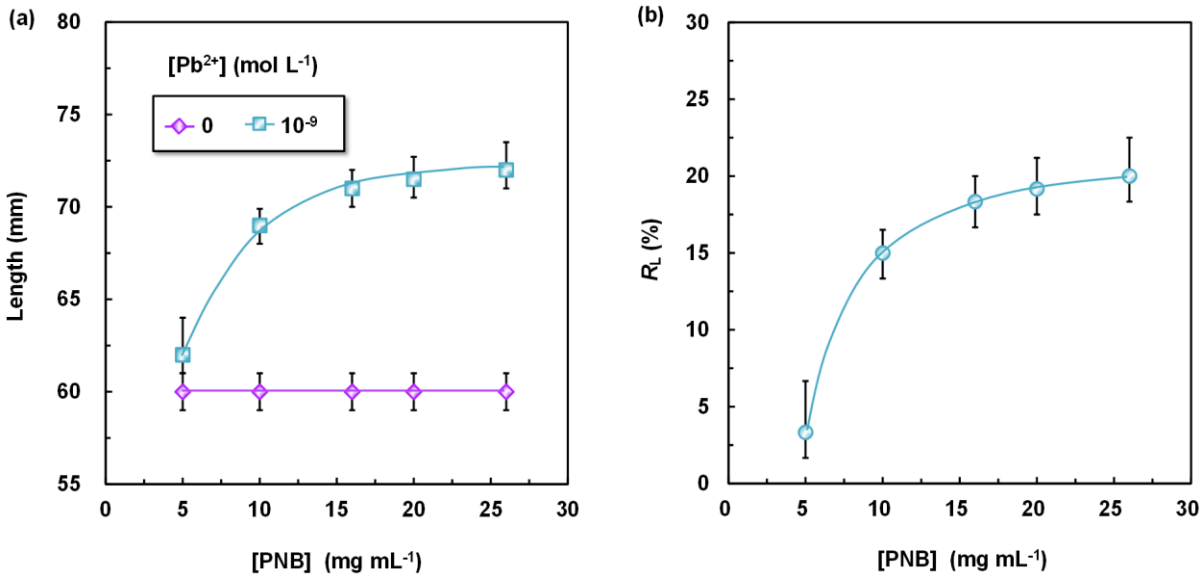

Fig. 9. Effect of the contents of PNB nanogels inside capsules on the Pb^{2+}-induced swelling ratios of capsule membrane groups. (a) Effect of the contents of PNB nanogels inside capsules on the total lengths of capsule membrane groups in pure water and aqua-solution with the value of $[Pb^{2+}]$ is 10^{-9} mol L^{-1}. (b) Effect of contents of PNB nanogels inside capsules on the length change ratios of capsule membrane groups in Pb^{2+}-containing solution with the value of $[Pb^{2+}]$ is 10^{-9} mol L^{-1}. T = 38 ℃.

3.7. Detection of the $[Pb^{2+}]$ value in water

For demonstration of facile detection of the $[Pb^{2+}]$ value in water, capsule membranes

encapsulated with 10 mg mL^{-1} PNB nanogels are prepared. The length change ratios of 15 capsule membranes in a line in aqueous solutions that contain Pb^{2+} are measured at 38 °C, with the $[Pb^{2+}]$ range of 10^{-9} ~ 10^{-6} mol L^{-1}. The results show that the total lengths of capsule membrane groups increase remarkably with increasing the $[Pb^{2+}]$ value, which can be easily observed by the naked eye (**Fig. 10**).

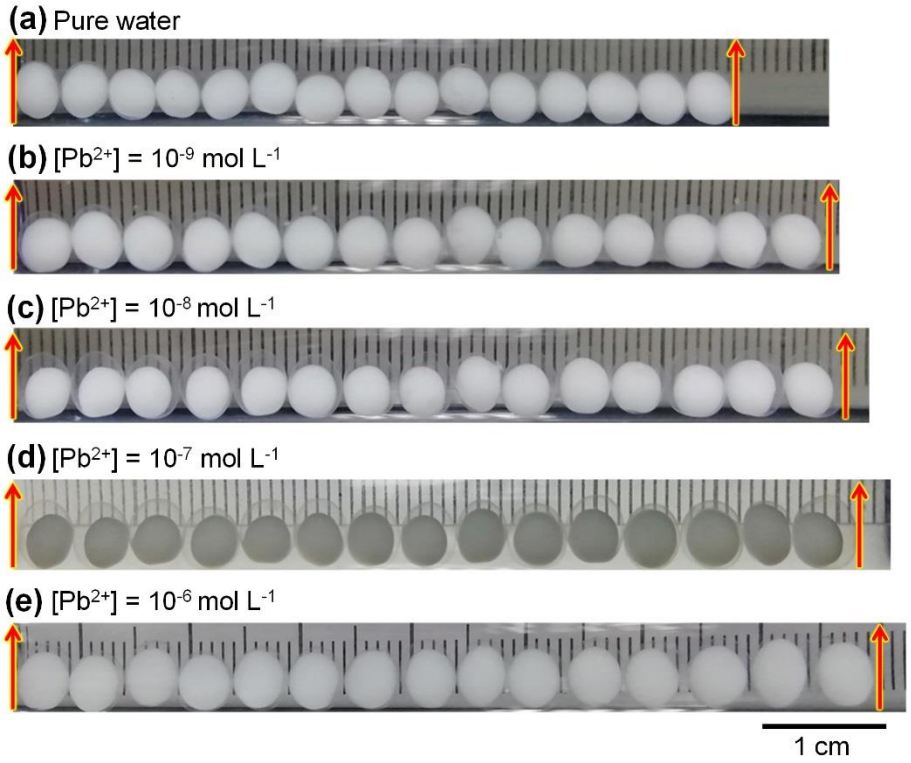

Fig. 10. Optical photographs of the capsule membrane groups for facile detection of $[Pb^{2+}]$. (a) Pure water, (b) $[Pb^{2+}] = 10^{-9}$ mol L^{-1}, (c) $[Pb^{2+}] = 10^{-8}$ mol L^{-1}, (d) $[Pb^{2+}] = 10^{-7}$ mol L^{-1}, (e) $[Pb^{2+}] = 10^{-6}$ mol L^{-1}. T = 38 ℃. The scale bar is 1 cm.

The dynamic changes of total lengths of capsule membrane groups after switching the environmental solution from pure water to aqueous solutions with different $[Pb^{2+}]$ values are shown in **Fig. 11a**. In pure water, the total length of the capsule membrane group does not

change at all. Nevertheless, when Pb^{2+} ions present in the above described environmental solutions, the total lengths of the capsule membrane groups increase gradually with increasing the immersing time, until the equilibrium of the osmotic pressures existed between inside and outside of the capsule membranes is reached. The time periods required to reach the equilibrium of osmotic pressures increase with increasing the $[Pb^{2+}]$. When the $[Pb^{2+}]$ values are 10^{-9}, 10^{-8}, 10^{-7} and 10^{-6} mol L^{-1}, the required time periods to reach the above-mentioned equilibrium are respectively about 40, 50, 60 and 60 min. The more the Pb^{2+} ions in environmental solution, the longer the time period needed for Pb^{2+} ions diffusing into capsule membranes to reach the equilibrium concentration.

At any given time, the length change ratio (R_L) of capsule membrane group increases with increasing the $[Pb^{2+}]$ value in a range of $10^{-9} \sim 10^{-6}$ mol L^{-1} (**Fig. 11b**). According to the results in **Fig. 11b**, for the R_L value after reaching equilibrium and the $[Pb^{2+}]$ value, a quantitative relationship can be summarized (**Fig. 11c**), and fits the following equation:

$$[Pb^{2+}] = 3\times10^{-21}\ R_L^{10.12} \quad (4)$$

With the help of Eq. (4), the concentration of trace Pb^{2+} ions in water with the $[Pb^{2+}]$ value ranging from 10^{-9} mol L^{-1} to 10^{-6} mol L^{-1} is able to be easily detected by directly measuring the Pb^{2+}-induced length change ratio of capsule membrane group after reaching equilibrium based on interpolation, which can be easily obtained by observing it simply by the naked eye before and after switching the environmental solution from pure water to Pb^{2+}-containing aqueous solution. Moreover, to further improve the measurement accuracy, the $[Pb^{2+}]$ can be determined by arranging more capsule membranes in a line to amplify the diameter change of capsules. However, compared with precision instruments such as Atomic Absorption Spectroscopy (AAS) and Inductively Coupled Plasma-Mass Spectrometry (ICP-MS), the detection accuracy of this capsule strategy is still limited. By this facile method, the approximate range of $[Pb^{2+}]$ can be

determined easily. Through the detection, the [Pb^{2+}] in water can be preliminarily confirmed in a range of 10^{-9} to 10^{-6} mol L^{-1}, which covers the maximum allowable [Pb^{2+}] in drinking water stipulated by the World Health Organization (*i.e.,* 4.83 × 10^{-8} mol L^{-1}) and the maximum allowable [Pb^{2+}] in industrial wastewater discharge standards (*i.e.,* 6.13 × 10^{-6} mol L^{-1}).

For the consideration of the effects of pH and ionic strength on the detection performances, owing to the carboxyl groups in alginate membranes and PNIPAM networks in nanogels, pH and ionic strength in water have certain effects on the swelling of nanogels and alginate membranes within a certain range. However, the main purpose of the proposed functional capsule membranes in this study is to develop a facile method and an easily portable tool for visually detecting trace [Pb^{2+}] in domestic water and drinking water, among which the pH value is not lower than 4 or higher than 7. The variation of pH values within this range in the Pb^{2+}-containing solution has nearly no obvious effect on PNB nanogels and alginate membranes [38-41]. Furthermore, the swelling of capsules and nanogels is nearly not affected by very low ion strength in domestic water and drinking water. However, for Pb^{2+}-containing solutions with high ion strength, the capsules may rupture owing to the ion exchange mechanism [42, 43]. Therefore, our proposed capsule membranes are designed to be mainly used for detection of trace [Pb^{2+}] in domestic water and drinking water. For the detection applications of Pb^{2+}-containing solutions with strong acidic/alkaline or high ion strength, further design and exploration of capsule membranes for [Pb^{2+}]-detection are needed.

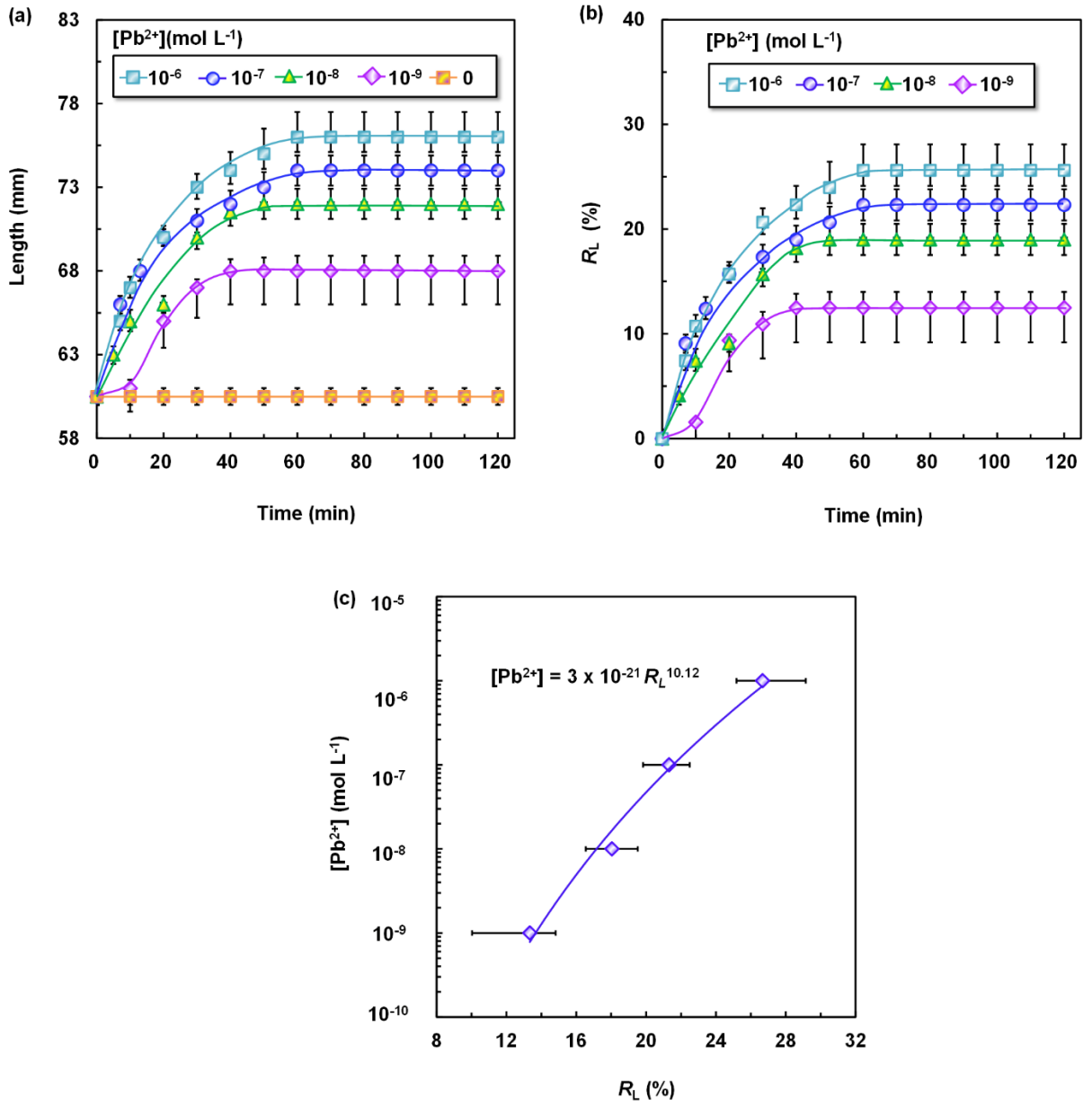

Fig. 11. Quantitative relationship between the swelling of capsule membrane group and the Pb^{2+} concentration in water. (a, b) Dynamic change of the total length (a) and the length change ratio (b) of capsule membrane group after switching the environmental solution from pure water to aqua-solutions containing Pb^{2+} with different $[Pb^{2+}]$ values. (c) Quantitative relationship between the length change ratio (R_L) of the capsule membrane group after reaching equilibrium and the $[Pb^{2+}]$ value in water. $T = 38$ °C.

4. Conclusions

In summary, a novel method based on capsule membranes encapsulated with smart nanogels has been developed for facilely detecting [Pb^{2+}] in water. The capsule membrane system is composed of a semi-permeable and elastic Ca-Alg membrane and encapsulated PNB nanogels that functionalized with 18-crown-6 crown ether units for specifically recognizing Pb^{2+} ions. The semi-permeable membrane allows Pb^{2+} ions and water to pass through quickly, but rejects the encapsulated nanogels and polymers totally. As soon as Pb^{2+} ions appear in the aqueous environment and enter into the capsule membrane, they can be specifically captured by the 18-crown-6 moieties existing on the PNB nanogels and cause the formation of 18-crown-6/Pb^{2+} complexes, leading to a Pb^{2+}-induced isothermal phase changing of encapsulated PNB nanogels from shrunken and hydrophobic state to swollen and hydrophilic state. Therefore, the osmotic pressure inside the capsule membrane increases remarkably, and thus the elastic capsule membrane isothermally swells upon the presence of Pb^{2+} ions in the environmental aqueous solution. And, the isothermal swelling degree of the prepared capsule membranes is dependent on the [Pb^{2+}] in water. Thus, the [Pb^{2+}] in water is able to be easily detected by directly measuring the Pb^{2+}-induced isothermal swelling ratio of the proposed capsule membrane. To amplify the Pb^{2+}-induced swelling effect, a group of 15 prepared capsule membranes are arranged in a line as a demonstration, and the Pb^{2+}-induced increase of the total length of the capsule membrane group is able to be easily observed by the naked eyes. With the capsule membrane group, the minimum concentration that can be easily detected in water is 10^{-9} mol L^{-1} in this work. Such a proposed strategy based on the capsule membranes encapsulated with smart nanogels provides a facile method and an easily portable tool for Pb^{2+}-detection, and it is also able to be applied to develop novel methods for facile detection of various chemical and/or

biological substances by introducing proper smart nanogels encapsulated in capsule membranes.

Acknowledgements

The authors gratefully acknowledge support from the National Natural Science Foundation of China (21991101), Fok Ying-Tung Education Foundation for Young Teachers in the Higher Education Institutions of China (151070) and Sichuan Provincial Youth Science and Technology Foundation (2017JQ0027).

References

[1] J.O. Nriagu, J.M. Pacyna, Quantitative assessment of worldwide contamination of air, water and soils by trace metals, Nature 333 (1988) 134-139.

[2] A. Roy, D. Bellinger, H. Hu, J. Schwartz, A.S. Ettinger, R.O. Wright, M. Bouchard, K. Palaniappan, K. Balakrishnan, Lead exposure and behavior among young children in Chennai, India, Environ. Health Perspect. 117 (2009) 1607-1611.

[3] H.R. Yu, J.Q. Hu, Z. Liu, X.J. Ju, R. Xie, W. Wang, L.Y. Chu, Ion-recognizable hydrogels for efficient removal of cesium ions from aqueous environment, J. Hazard. Mater. 323 (2017) 632-640.

[4] D.A. Gidlow, Lead toxicity, Occup. Med. 54 (2004) 76-81.

[5] M. Hanna-Attisha, J. Lachance, R.C. Sadler, S. Champney, Elevated blood lead levels in children associated with the Flint drinking water crisis: A spatial analysis of risk and public health response, Am. J. Public Health 106 (2016) 283-290.

[6] R. Baum, J. Bartram, S. Hrudey, The Flint water crisis confirms that U.S. drinking water needs improved risk management, Environ. Sci. Technol. 50 (2016) 5436-5437.

[7] D.C. Bellinger, Lead contamination in Flint- an abject failure to protect public health, N.

Engl. J. Med. 374 (2016) 1101-1103.

[8] S. Caroli, G. Forte, A.L. Iamiceli, B. Galoppi, Determination of essential and potentially toxic trace elements in honey by inductively coupled plasma-based techniques, Talanta 50 (1999) 327-336.

[9] S. Ashoka, B.M. Peake, G. Bremner, K.J. Hageman, M.R. Reid, Comparison of digestion methods for ICP-MS determination of trace elements in fish tissues, Anal. Chim. Acta 653 (2009) 191-199.

[10] I. Narin, M. Soylak, L. Elci, M. Dogan, Determination of trace metal ions by AAS in natural water samples after preconcentration of pyrocatechol piolet complexes on an activated carbon column, Talanta 52 (2000) 1041-1046.

[11] M.E. Mahmoud, I.M.M. Kenawy, M.A.H. Hafez, R.R. Lashein, Removal, preconcentration and determination of trace heavy metal ions in water samples by AAS via chemically modified silica gel N-(1-carboxy-6-hydroxy) benzylidenepropylamine ion exchanger, Desalination 250 (2010) 62-70.

[12] I.K. Tonlé, S. Letaief, E. Ngameni, A. Walcarius, C. Detellier, Square wave voltammetric determination of lead(II) ions using a carbon paste electrode modified by a thiol‐functionalized kaolinite, Electroanalysis 23 (2011) 245-252.

[13] A. Döring, W. Birnbaum, D. Kuckling, Responsive hydrogels-structurally and dimensionally optimized smart frameworks for applications in catalysis, micro-system technology and material science, Chem. Soc. Rev. 42 (2013) 7391-7420.

[14] L.Y. Chu, R. Xie, X.J. Ju, W. Wang, Smart hydrogel functional materials, Springer, Berlin, 2014.

[15] S. Lin, W. Wang, X.J. Ju, R. Xie, Z. Liu, H.R. Yu, C. Zhang, L.Y. Chu, Ultrasensitive

microchip based on smart microgel for real-time online detection of trace threat analytes., Proc. Natl.Acad. Sci. U. S. A. 113 (2016) 2023-2028.

[16] Z. Liu, F. Luo, X.J. Ju, R. Xie, Y.M. Sun, W. Wang, L.Y. Chu, Gating membranes for water treatment: detection and removal of trace Pb^{2+} ions based on molecular recognition and polymer phase transition, J. Mater. Chem. A 1 (2013) 9659-9671.

[17] Y. Wang, Z. Liu, H.Y. Peng, F. He, L. Zhang, Y. Faraj, W. Wang, X.J. Ju, R. Xie, L.Y. Chu, A simple device based on smart hollow microgels for facile detection of trace lead(II) ions, Chemphyschem 19 (2018) 2025-2036.

[18] P.J. Yan, F. He, W. Wang, S.Y. Zhang, L. Zhang, M. Li, Z. Liu, X.J. Ju, R. Xie, L.Y. Chu, Novel membrane detector based on smart nanogels for ultrasensitive detection of trace threat substances, ACS Appl. Mater. Interfaces 10 (2018) 36425-36434.

[19] A. Matsumoto, N. Sato, T. Sakata, R. Yoshida, K. Kataoka, Y. Miyahara, Chemical-to-electrical-signal transduction synchronized with smart gel volume phase transition, Adv. Mater. 21 (2010) 4372-4378.

[20] M. Guenther, D. Kuckling, C. Corten, G. Gerlach, J. Sorber, G. Suchaneck, K.F. Arndt, Chemical sensors based on multiresponsive block copolymer hydrogels, Sensors & Actuators: B. Chemical 126 (2007) 97-106.

[21] Z.E. Jacobi, L. Li, J.W. Liu, Visual detection of lead(II) using a label-free DNA-based sensor and its immobilization within a monolithic hydrogel, Analyst 137 (2012) 704-709.

[22] Y.X. Yuan, Z.L. Li, Y. Liu, J.P. Gao, Z. Pan, Y. Liu, Hydrogel photonic sensor for the detection of 3-pyridinecarboxamide, Chemistry 18 (2012) 303-309.

[23] W. Hong, W.H. Li, X.B. Hu, B.Y. Zhao, F. Zhang, D. Zhang, Highly sensitive colorimetric sensing for heavy metal ions by strong polyelectrolyte photonic hydrogels, .J. Am. Chem. Soc. 21 (2011) 17193-17201.

[24] Y.J. Zhao, X.W. Zhao, B.C. Tang, W.Y. Xu, J. Li, H. Jing, Z.Z. Gu, Quantum‐dot‐tagged bioresponsive hydrogel suspension array for multiplex label‐free DNA detection, Adv. Funct. Mater. 20 (2010) 976-982.

[25] G. Ye, C.Q. Yang, X.G. Wang, Sensing diffraction gratings of antigen-responsive hydrogel for human immunoglobulin-g detection, Macromol. Rapid Commun. 31 (2010) 1332-1336.

[26] K. Liu, H.F. Ji, Detection of Pb^{2+} using a hydrogel swelling microcantilever sensor, Anal. Sci. 75 (2004) 9-11.

[27] Q.F. Luo, Y. Guan, Y.J. Zhang, M. Siddiq, Lead-sensitive PNIPAM microgels modified with crown ether groups, J. Polym. Sci., Part A: Polym. Chem. 48 (2010) 4120-4127.

[28] X.Q. Wang, Y. Gang, X.G. Wang, Hydrogel diffraction gratings functionalized with crown ether for heavy metal ion detection, Sens. Actuators, B 193 (2014) 413-419.

[29] H.Y. Peng, W. Wang, F.H. Gao, S. Lin, L.Y. Liu, X.Q. Pu, Z. Liu, X.J. Ju, R. Xie, L.Y. Chu, Ultrasensitive diffraction gratings based on smart hydrogels for highly selective and rapid detection of trace heavy metal ions, J. Mater. Chemistry C 6 (2018) 11356-11367

[30] A.L. Chen, H.R. Yu, X.J. Ju, R. Xie, W. Wang, L.Y. Chu, Visual detection of lead(II) using a simple device based on P(NIPAM-co-B18C6Am) hydrogel, RSC Adv. 4 (2014) 26030-26037.

[31] M.Y. Jiang, X.J. Ju, L. Fang, Z. Liu, H.R. Yu, L. Jiang, W. Wang, R. Xie, Q. Chen, L.Y. Chu, A novel, smart microsphere with K^+ induced shrinking and aggregating properties based on a responsive host-guest system, ACS Appl. Mater. Interfaces 6 (2014) 19405-19415.

[32] J.Y. Wang, Y. Jin, R. Xie, J.Y. Liu, X.J. Ju, T. Meng, L.Y. Chu, Novel calcium-alginate capsules with aqueous core and thermo-responsive membrane, J. Colloid Interface Sci. 353 (2011) 61-68.

[33] X.J. Ju, S.B. Zhang, M.Y. Zhou, R. Xie, L.H. Yang, L.Y. Chu, Novel heavy-metal adsorption material: ion-recognition P(NIPAM-co-BCAm) hydrogels for removal of lead(II) ions, J. Hazard. Mater. 167 (2009) 114-118.

[34] X.J. Ju, L. Liu, R. Xie, C.H. Niu, L.Y. Chu, Dual thermo-responsive and ion-recognizable monodisperse microspheres, Polymer 50 (2009) 922-929.

[35] B. Zhang, X.J. Ju, R. Xie, Z. Liu, S.W. Pi, L.Y. Chu, Comprehensive effects of metal ions on responsive characteristics of P(NIPAM-co-B18C6Am), J. Phys. Chem. B 116 (2012) 5527-5536.

[36] R.M. Izatt, R.E. Terry, B.L. Haymore, L.D. Hansen, N.K. Dalley, A.G. Avondet, J.J. Christensen, Calorimetric titration study of the interaction of several uni- and bivalent cations with 15-crown-5, 18-crown-6, and two isomers of dicyclohexo-18-crown-6 in aqueous solution at 25 °C and μ=0.1., J. Am. Chem. Soc. 98 (1977) 7620-7626.

[37] T. Yamaguchi, T. Ito, T. Sato, T. Shinbo, S.I. Nakao, Development of a fast response molecular recognition ion gating membrane, J. Am. Chem. Soc. 121 (1999) 4078-4079.

[38] Y.M. Liu, X.J. Ju, Y. Xin, W.C. Zheng, W. Wang, J. Wei, R. Xie, Z. Liu, L.Y. Chu, A novel smart microsphere with magnetic core and ion-recognizable shell for Pb^{2+} adsorption and separation, ACS Appl. Mater. Interfaces 6 (2014) 9530-9542.

[39] X.B. Luo, L.L. Liu, F. Deng, S.L. Luo, Novel ion-imprinted polymer using crown ether as a functional monomer for selective removal of Pb(II) ions in real environmental water samples, J. Mater. Chem. A 1 (2013) 8280-8286.

[40] G.E. Morris, B. Vincent, M.J. Snowden, Adsorption of lead Ions onto *N*-isopropylacrylamide and acrylic acid copolymer microgels, J. Colloid Interface Sci. 190 (1997) 198-205.

[41] F. He, L. Mei, X.J. Ju, R. Xie, W. Wang, Z. Liu, F. Wu, L.Y. Chu, pH-responsive controlled release characteristics of solutes with different molecular weights diffusing across

membranes of Ca-alginate/protamine/silica hybrid capsules, J. Membr. Sci. 474 (2015) 233-243.

[42] L. Rolland, E. Santanach-Carreras, T. Delmas, J. Bibette, N. Bremond, Physicochemical properties of aqueous core hydrogel capsules, Soft Matter 10 (2014) 9668-9674.

[43] Q.F. Luo, Y. Guan, Y.J. Zhang, M. Siddiq, Lead-sensitive PNIPAM microgels modified with crown ether groups, J. Polym. Sci. Pol. Chem. 48 (2010) 4120-4127.